Electronic Supplementary Information

An anionic zeolite-like metal-organic framework (AZMOF) with Moravia network for organic dyes absorption through cation-exchange

Yu Shen,[a] Cong-Cong Fan,[a] Yu-Zhen Wei,[a] Jie Du,[a] Hai-Bin Zhu,[*a] and Yue Zhao[*b]

[a] *School of Chemistry and Chemical Engineering, Southeast University, Nanjing 211189 China. E-mail: zhuhaibin@seu.edu.cn*

[b] *Coordination Chemistry Institute, State Key Laboratory of Coordination Chemistry, School of Chemistry and Chemical Engineering, Nanjing National Laboratory of Microstructures, Nanjing University, Nanjing 210093, China. E-mail: zhaoyue@nju.edu.cn*

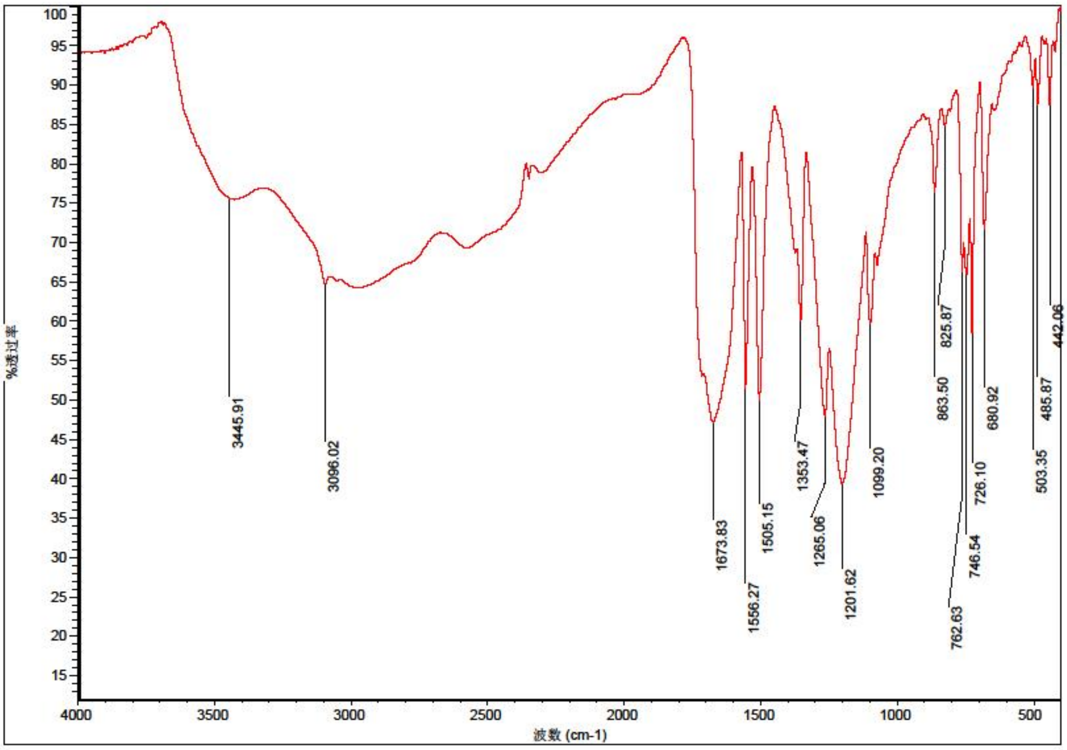

Fig. S1 FT-IR spectra of H_3BTTC

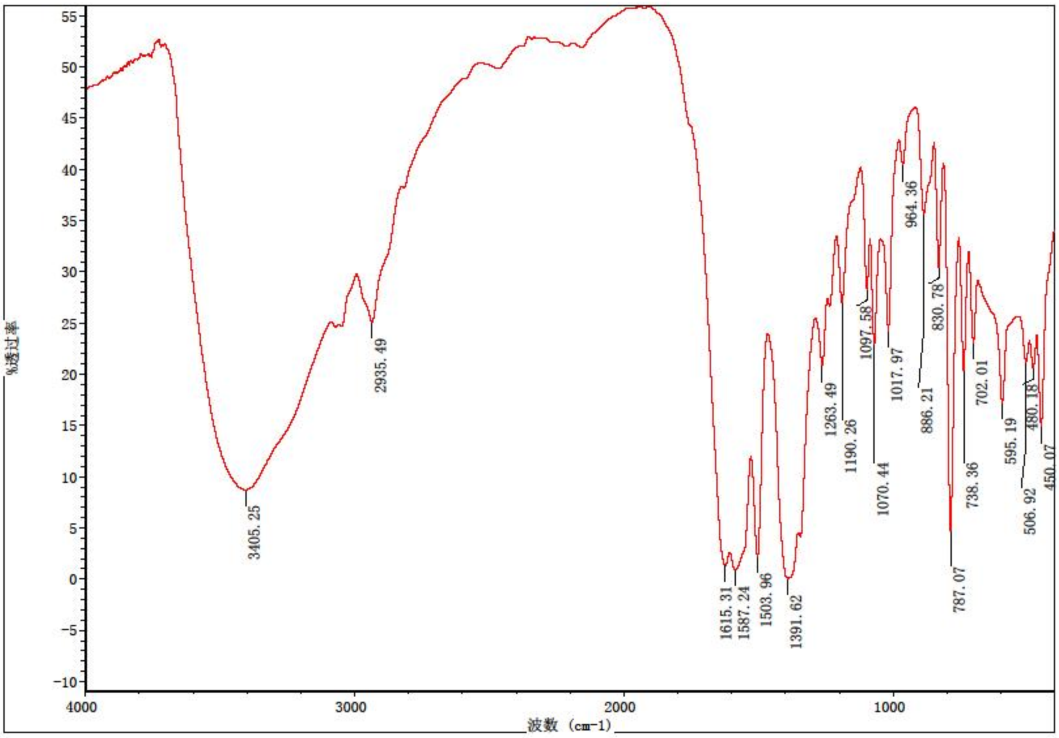

Fig. S2 FT-IR spectra of **Sr-BTTC**

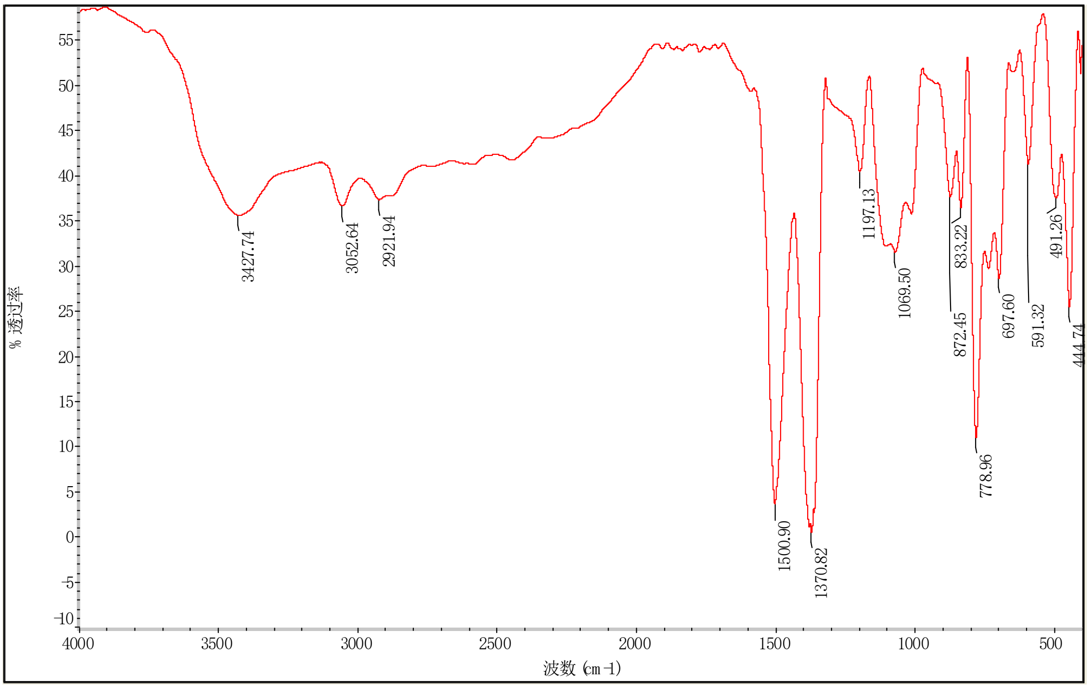

Fig. S3 FT-IR spectra of desolvated **Sr-BTTC** samples.

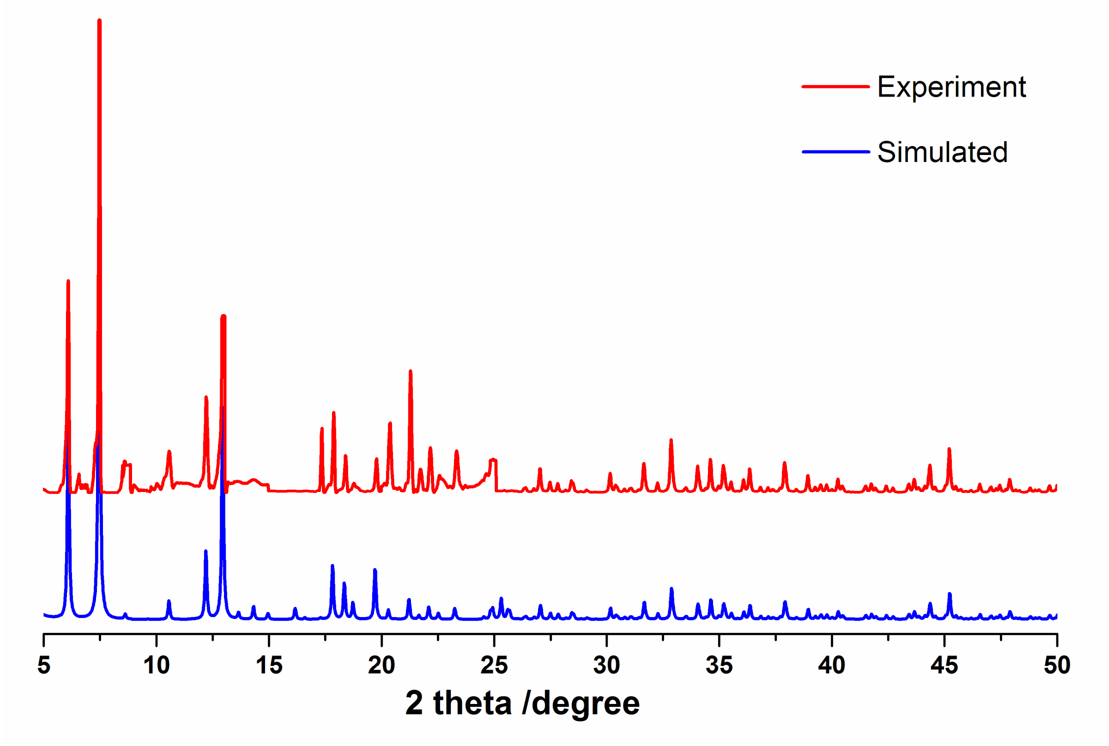

Fig. S4 PXRD pattern of **Sr-BTTC**

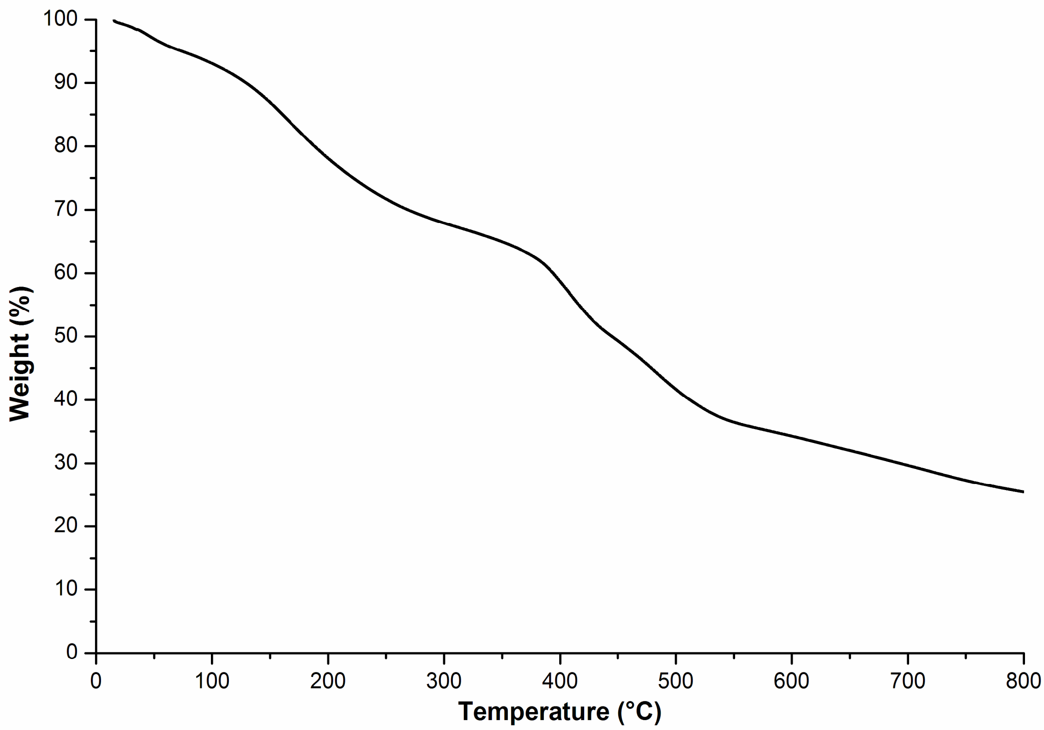

Fig. S5 TG curve of **Sr-BTTC:** The weight loss before 100 °C is contributed by the guest solvents, when the temperature was raised above 120 °C a substantial mass reduction was observed, which is possibly resulted by removal of coordinated water and terthienobenzene unit as the consequence of BTTC decarboxylation [1]

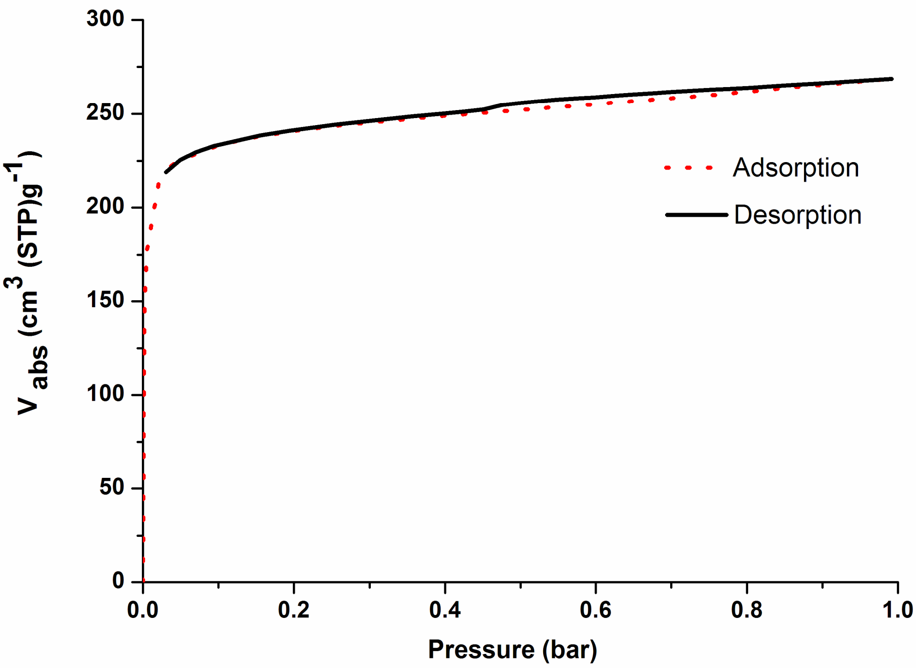

Fig. S6 N_2 sorption isotherm for **Sr-BTTC** recorded at 77K.

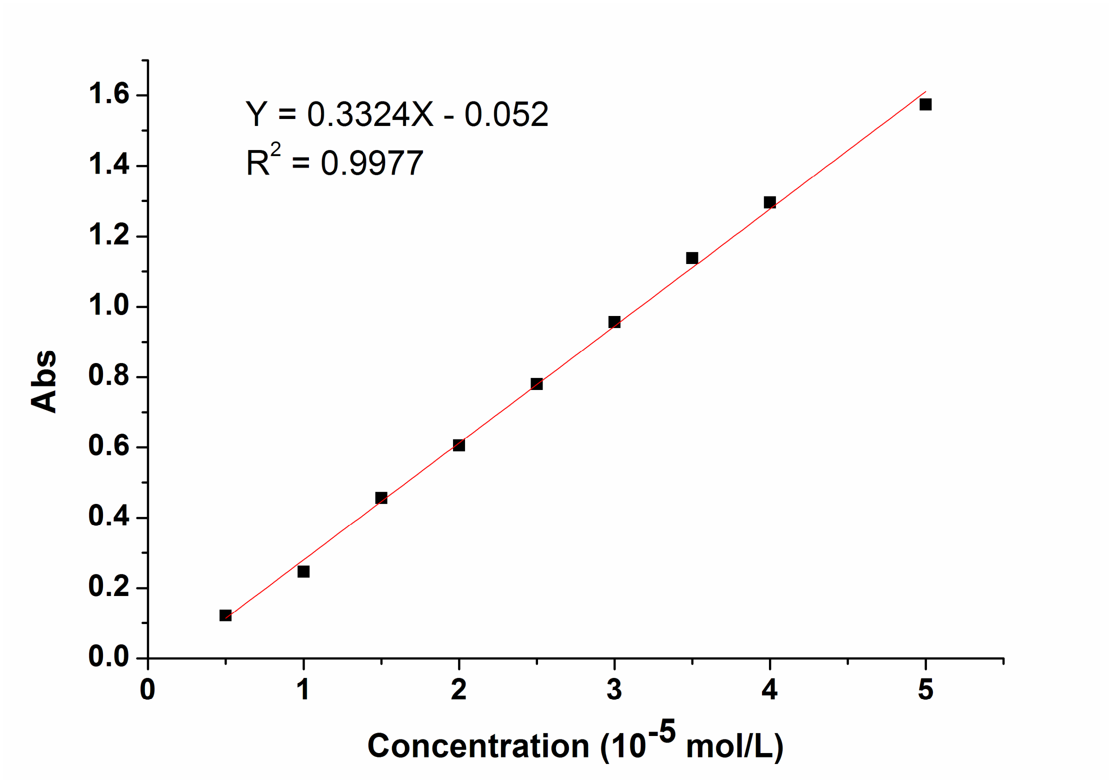

Fig. S7 The absorption intensity (black dots) of MB dye at different concentrations (mol/L) (The red solid line represents the best linear fit.)

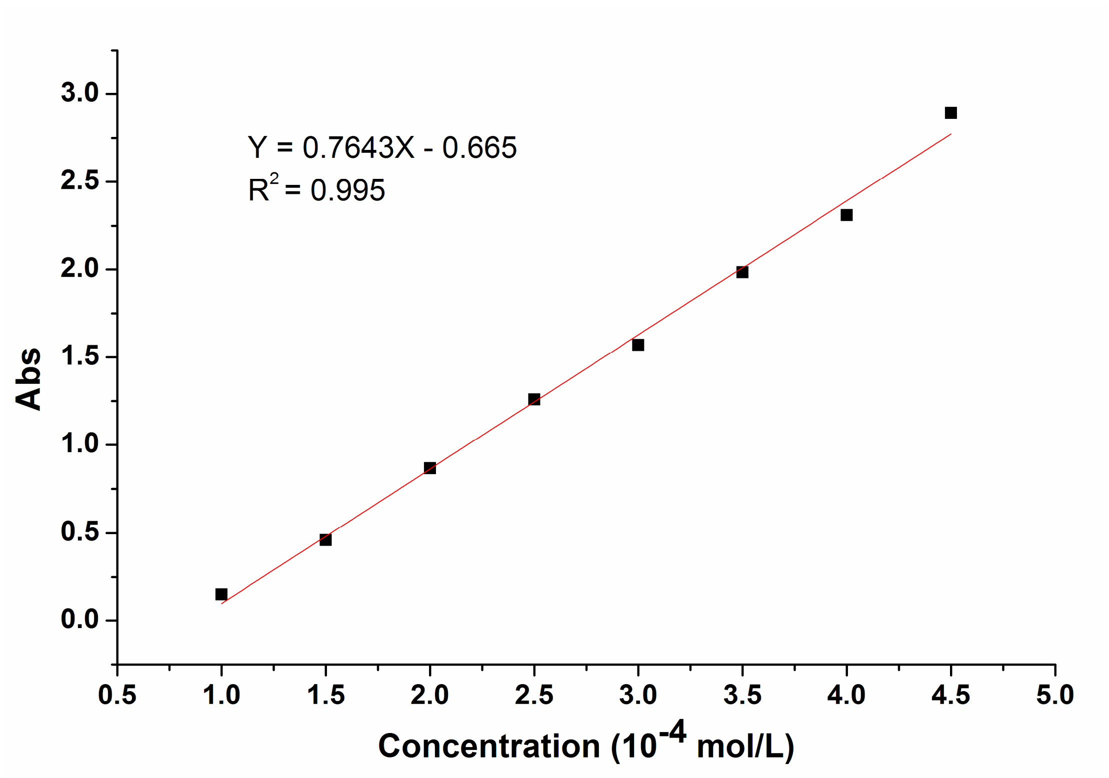

Fig. S8 The absorption intensity (black dots) of BR2 dye at different concentrations (mol/L)(The red solid line represents the best linear fit.)

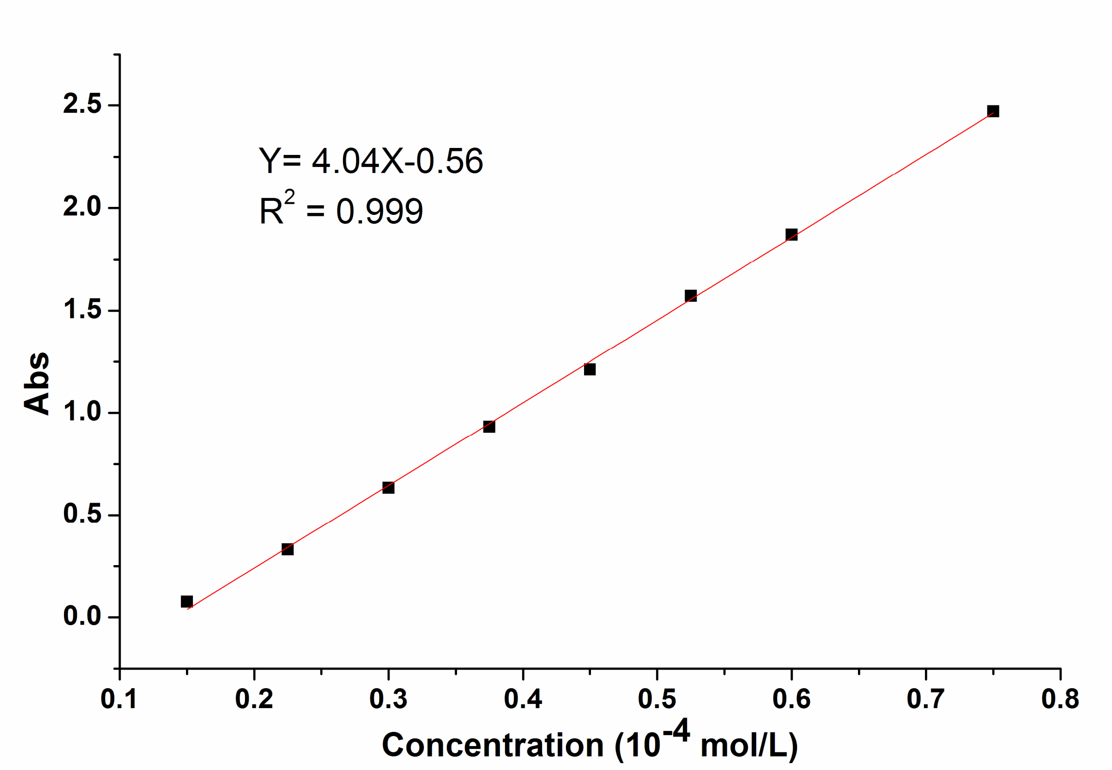

Fig. S9 The absorption intensity (black dots) of RB dye at different concentrations (mol/L)(The red solid line represents the best linear fit)

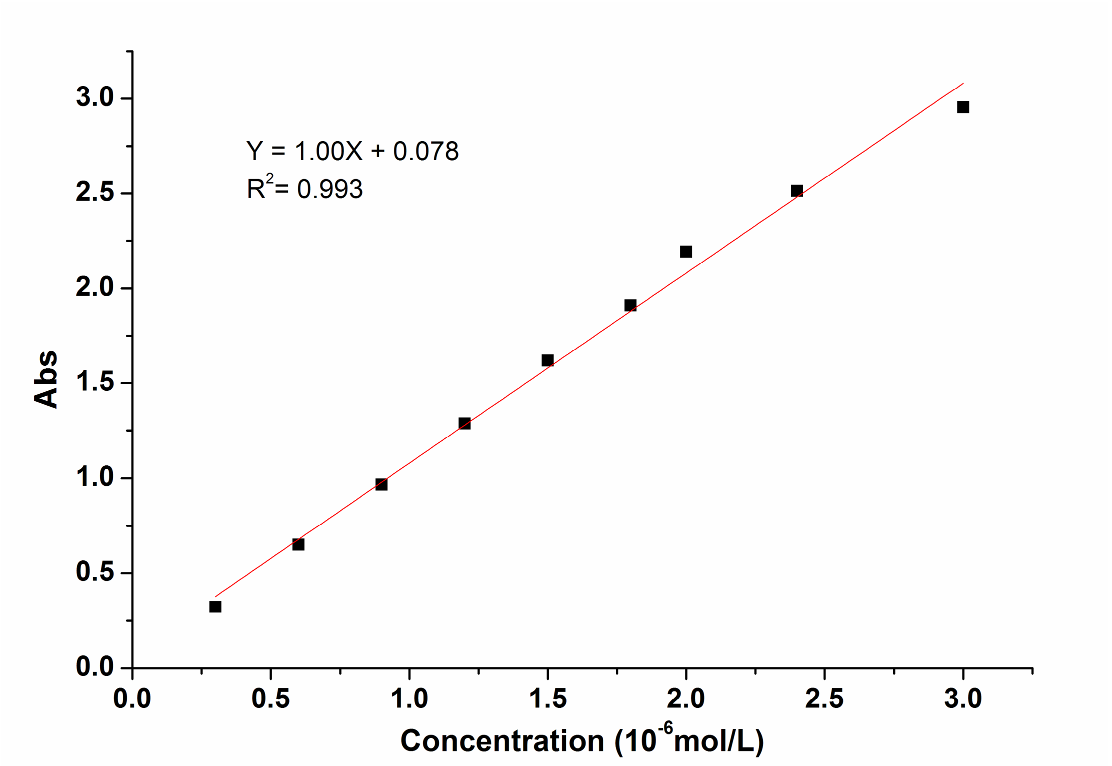

Fig. S10 The absorption intensity (black dots) of CV dye at different concentrations (mol/L)(The red solid line represents the best linear fit)

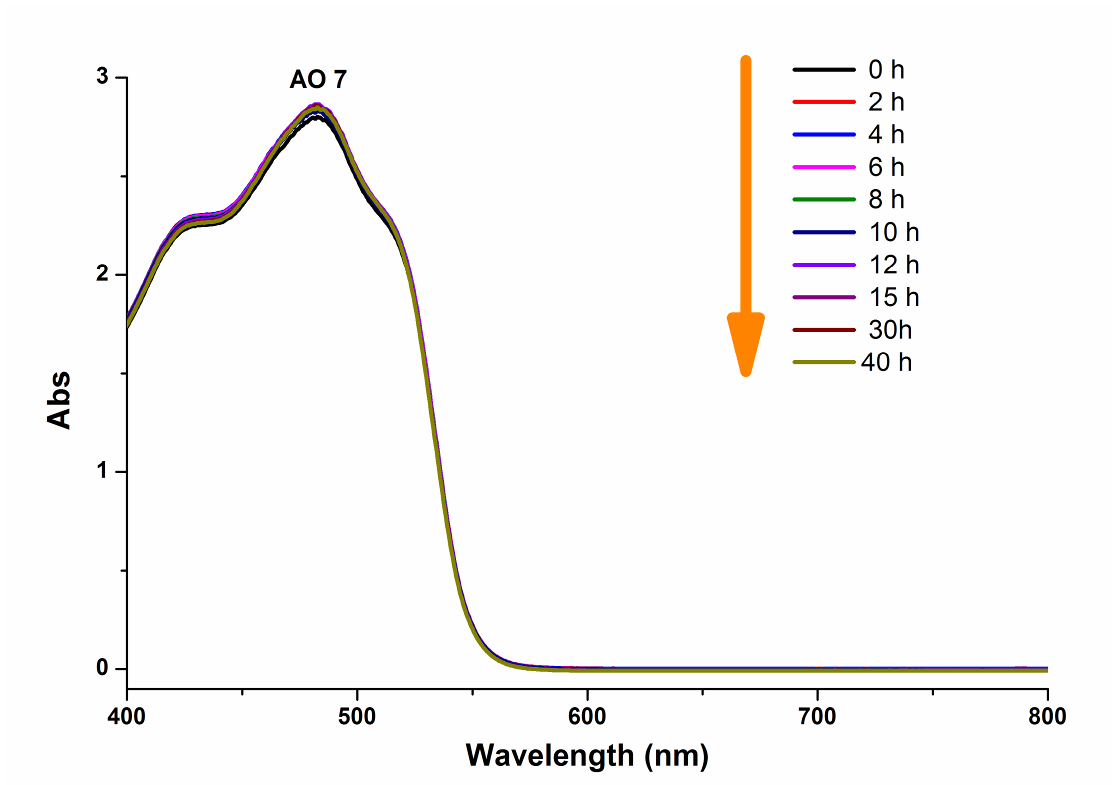

Fig. S11 The UV-Vis absorption change of AO7 in the presence of **Sr-BTTC**

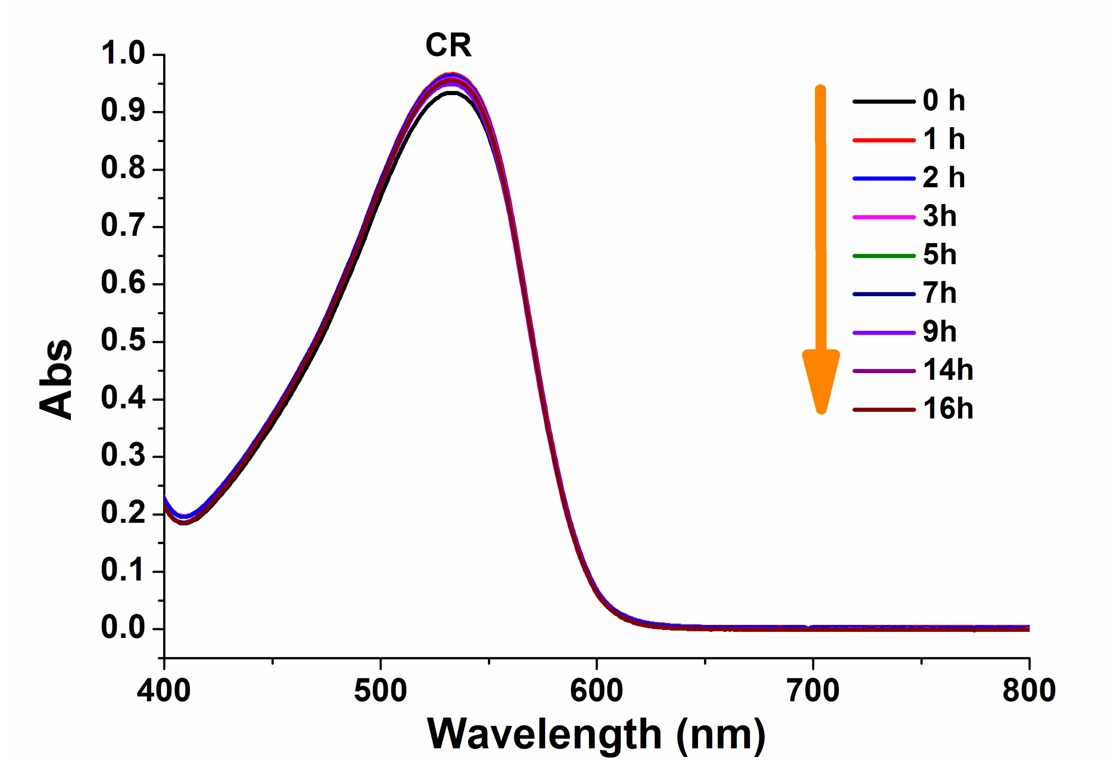

Fig. S12 The UV-Vis absorption change of CR in the presence of **Sr-BTTC**

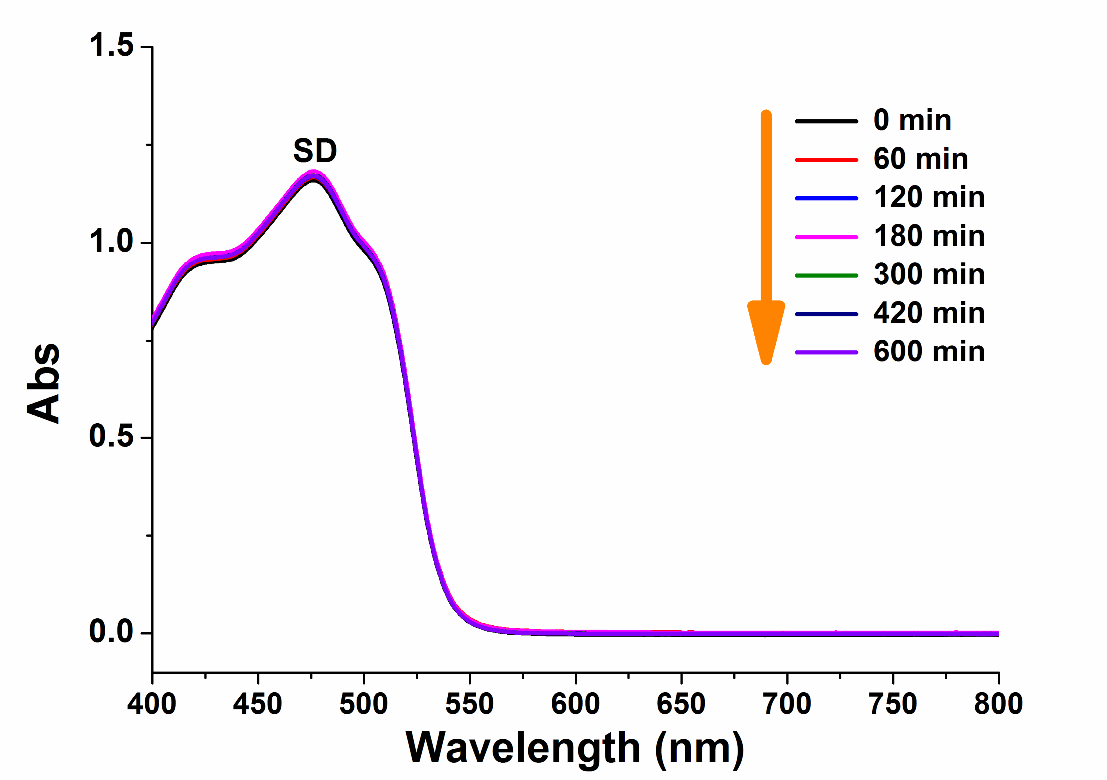

Fig. S13 The UV-Vis absorption change of CR in the presence of **Sr-BTTC**

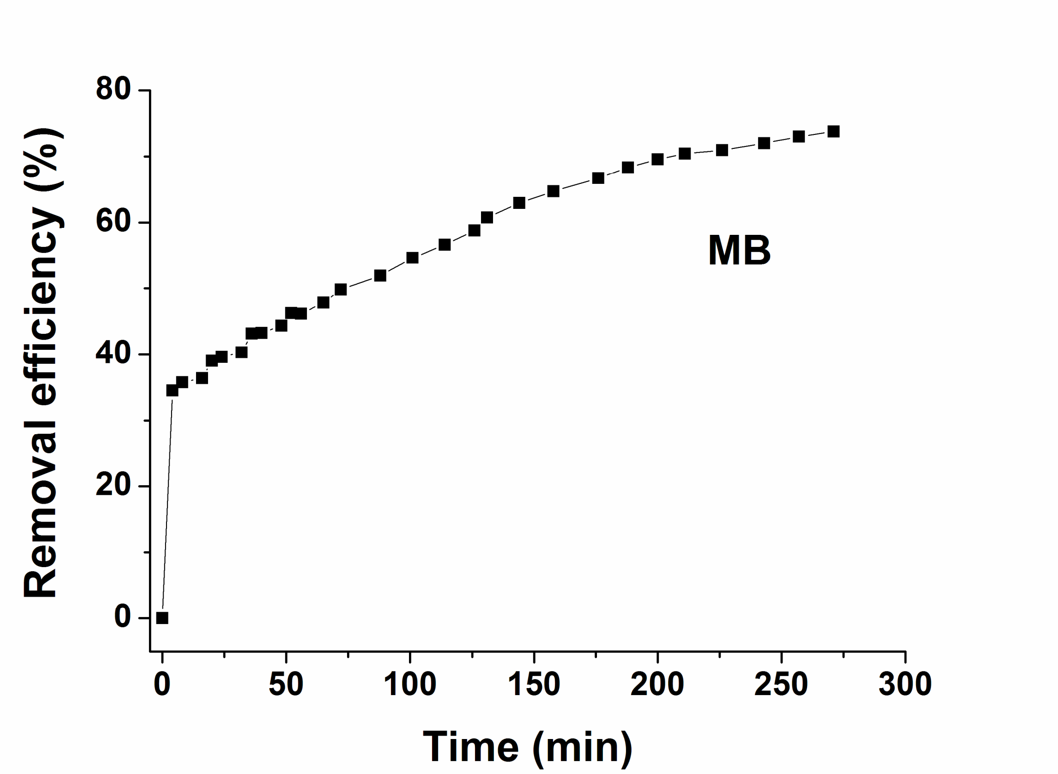

Fig. S14 Removal efficiency of MB in the presence of the **Sr-BTTC** with increasing time.

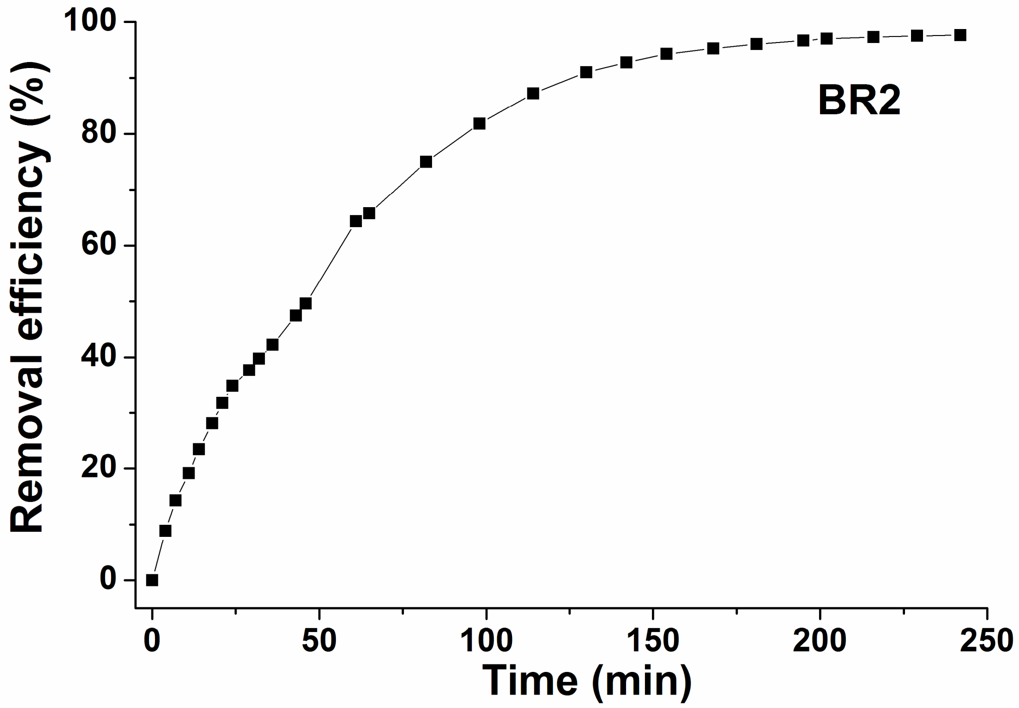

Fig. S15 Removal efficiency of BR2 in the presence of the **Sr-BTTC** with increasing time.

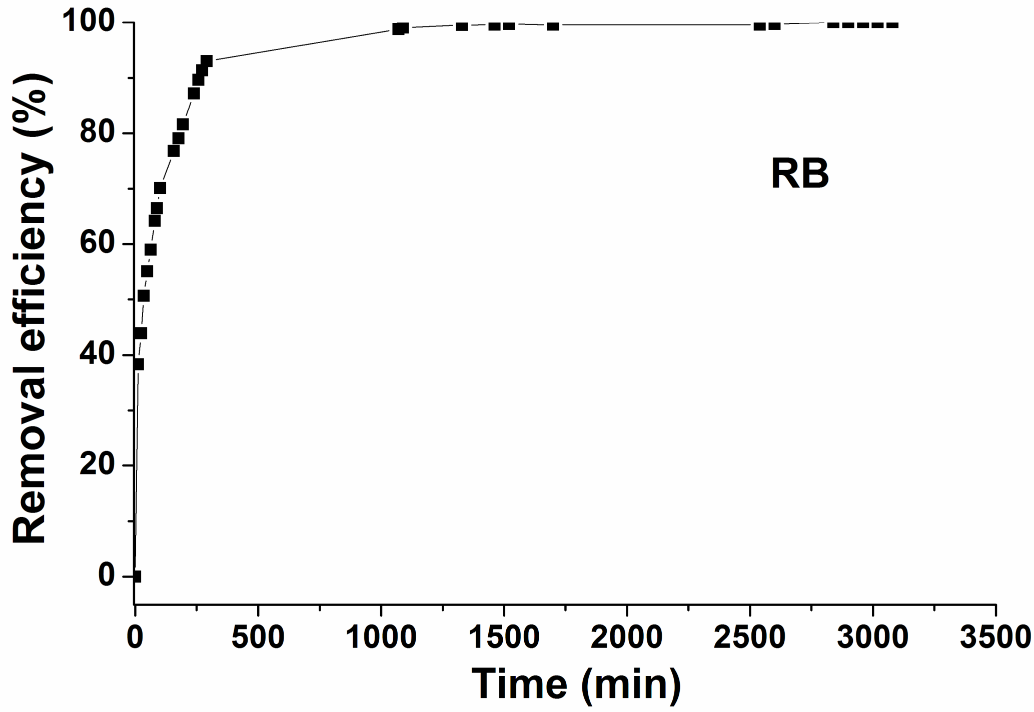

Fig. S16 Removal efficiency of RB in the presence of the **Sr-BTTC** with increasing time.

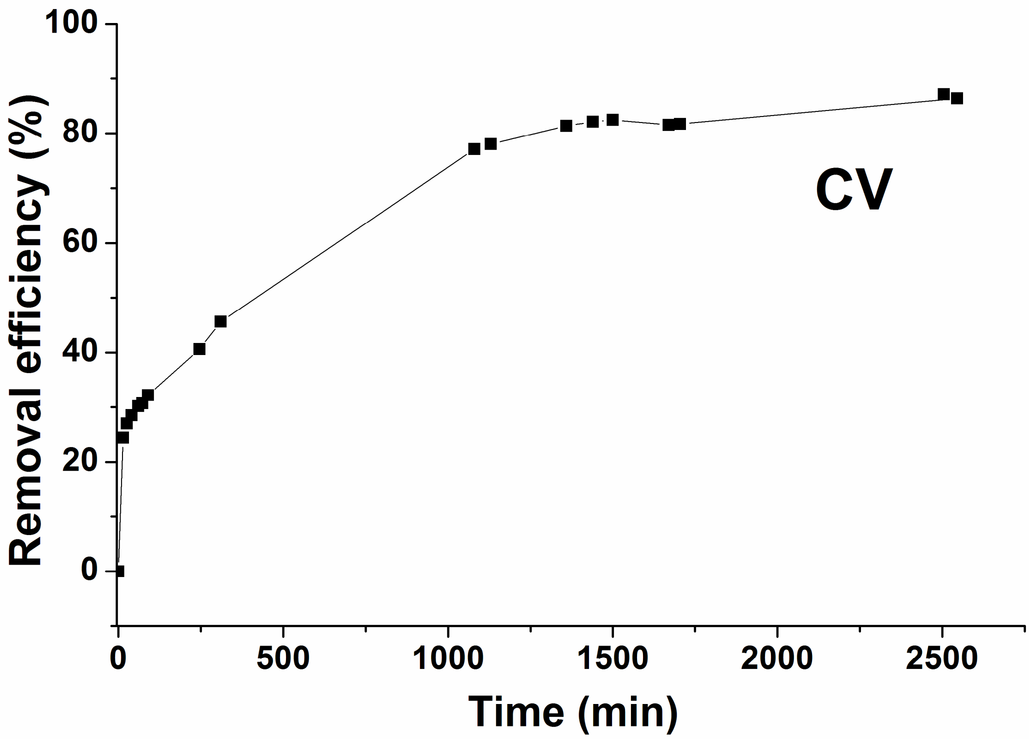

Fig. S17 Removal efficiency of CV in the presence of the **Sr-BTTC** with increasing time.

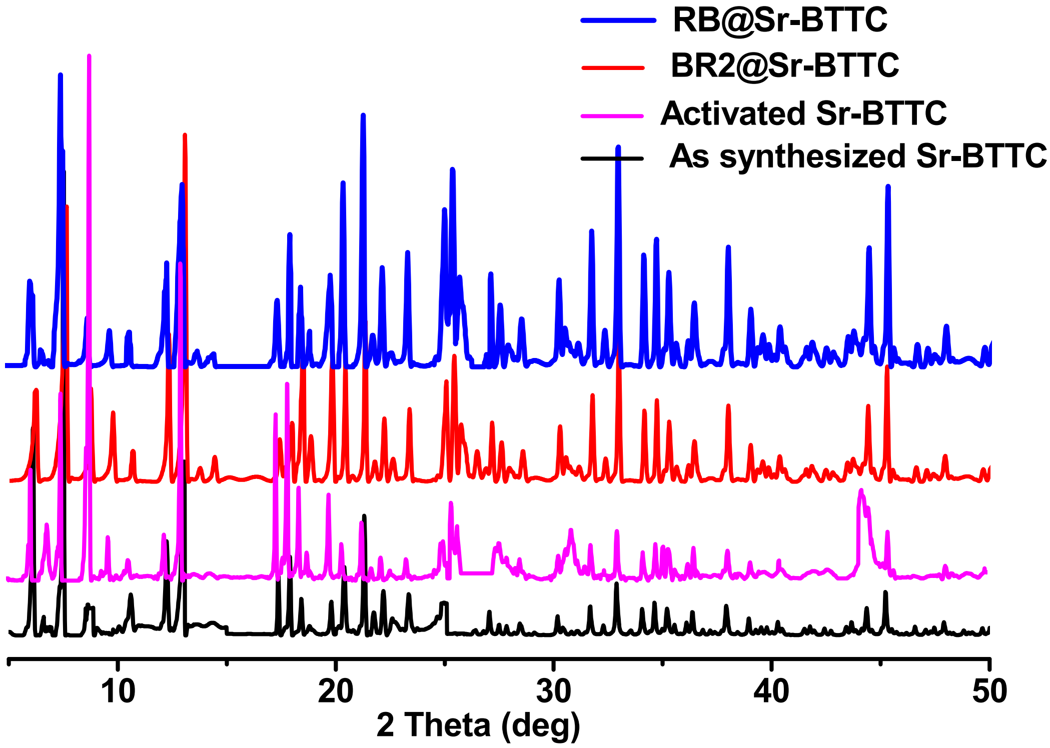

Fig. S18 PXRD patterns of as-synthesized **Sr-BTTC**, activated **Sr-BTTC** and dye-absorbed **Sr-BTTC**.

Table S1 Crystal data and structure refinements for **Sr-BTTC**

Compound	**Sr-BTTC**
Formula	$C_{960}H_{192}O_{552}S_{192}Sr_{104}$
Crystal size(mm)	0.28 × 0.25 × 0.22
T/K	293(2)
Crystal system	Cubic
Space group	*Fm-3c*
a (Å)	41.0051(9)
b (Å)	41.0051(9)
c (Å)	41.0051(9)
α (°)	90.00
β (°)	90.00
γ (°)	90.00
V (Å^3)	68947(5)
Z	1
D_c (g.cm^{-3})	0.863
F(000)	17392
Theta range/°	2.25 to 25.50
Reflections collected	48727
Unique reflections	2671
Goof	1.853
R_1^a [I > 2σ(I)]	0.0859
wR_2^b [I > 2σ(I)]	0.2517

[a] $R_1 = \Sigma||F_o| - |F_c||/\Sigma|F_o|$. [b] $wR_2 = |\Sigma w(|F_o|^2 - |F_c|^2)|/\Sigma|w(F_o^2)^2|^{1/2}$,
where $w = 1/[\sigma^2(F_o^2) + (aP)^2 + bP]$. $P = (F_o^2 + 2F_c^2)/3$.

Table S2 The adsorption capacity for BR on various adsorbents.

Adsorbents	Adsorption capacity (mg/g)	References
Sr-BTTC	**675**	**This work**
UiO-66-15	366	*Chem. Eng. J.*, 2016, **289**, 486-493
UiO-66-ND	39	*Chem. Eng. J.*, 2016, **289**, 486-493
Fly ash	7	*J. Hazard. Mater.*, 2011, **187**, 562-573
PET depolymerization products	29	*Clean-Soil Air Water.*, 2012, **40**, 325-333
Calcite	37.2	*Separ. Sci. Technol.*, 2010, **45**, 1471-1481
HT-SDBS	40.5	*J. Hazard. Mater.*, 2008, **153**, 911-918
HT-SDS	83.3	*J. Hazard. Mater.*, 2008, **153**, 911-918
Dairy sludge	95.2	*J. Environ. Eng. Sci.*, 2008, **7**, 433-438
Sulfonated Phenol-Formaldehyde Resin	103	*J. Appl. Polym. Sci.*, 2008, **109**, 2774-2780
Jalshakti	181.8	*Bioresour. Technol.*, 2006, **97**, 877-885
G-SO3H/Fe3O4	199.3	*Clean-Soil Air Water.*, 2013, **41**, 992-1001
starch-graft -AA	204	*J. Appl. Polym. Sci.*, 2007, **106**, 2422-2426
Rice husk carbon	294.1	*Indian. J. Chem. Techn.*, 2001, **8**, 133-139
Aluminium Pillared Clay	338	*Colloids Surfaces A.*, 2010, **366**, 88-94
AAm-AMPSNa-clay hydrogel nanocomposites	484.2	*Polym. Adv. Technol.*, 2008, **19**, 838-845.

Olive stone	526.3	*J. Hazard. Mater.*, 2009, **163**, 441-447
N-Vinyl 2-pyrrolidone/itaconic acid/organo clay nanocomposite hydrogel	550.0	*Water Air Soil Pollut.*, 2013, **224**, 1760-1775
Treated spent bleaching earth	555.6	*J. Colloid Interface Sci.*, 2007, **307**, 9-16

Table S3 The adsorption capacity for RB on various adsorbents.

Adsorbents	Adsorption capacity (mg/g)	References
Sr-BTTC	**545**	**This work**
TA-G	201	*Colloids Surf. A*, 2015, **477**, 35–41
Fe_3O_4 nanoparticles	161.8	*J. Hazard. Mater.*, 2012, **209–210**, 193–198
kaolinite	46.08	*Appl. Clay Sci.*, 2012, **69**, 58-66
Coconut (Cocos nucifera)	71	*J. Hazard. Mater.*, 2008, **158**, 65-72
Rice husk ash	13.76	*J. Environ. Manage.*, 2007, 84, 390-400
Cocoa (Theobroma cacao) shell	41	*Int. J. Eng. Sci. Technol.*, 2010, **2**, 6284-6292
Perlite	67	*J. Mater. Environ. Sci.*, 2012, **3**, 157-170
NiO	111	*Process Saf. Environ. Prot.*, 2015, **93**, 282-292

Reference:

[1]. D. Yuan, D. Zhao, D. J. Timmons and H.-C. Zhou, *Chem. Sci.*, 2011, **2**, 103-106.